



HAL
open science

Impact of forest fire on the mercury stable isotope composition in litter and soil in the Amazon

Larissa Richter, David Amouroux, Emmanuel Tessier, Anne H el ene Fostier

► To cite this version:

Larissa Richter, David Amouroux, Emmanuel Tessier, Anne H el ene Fostier. Impact of forest fire on the mercury stable isotope composition in litter and soil in the Amazon. *Chemosphere*, 2023, 339, pp.139779. 10.1016/j.chemosphere.2023.139779 . hal-04189575

HAL Id: hal-04189575

<https://univ-pau.hal.science/hal-04189575>

Submitted on 28 Nov 2023

HAL is a multi-disciplinary open access archive for the deposit and dissemination of scientific research documents, whether they are published or not. The documents may come from teaching and research institutions in France or abroad, or from public or private research centers.

L'archive ouverte pluridisciplinaire **HAL**, est destin ee au d ep ot et  a la diffusion de documents scientifiques de niveau recherche, publi es ou non,  emanant des  tablissements d'enseignement et de recherche fran ais ou  trangers, des laboratoires publics ou priv es.

Chemosphere

Impact of forest fire on the mercury stable isotope composition in litter and soil in the Amazon

--Manuscript Draft--

Manuscript Number:	
Article Type:	VSI:Latin-Analytical
Section/Category:	Environmental Chemistry
Keywords:	Isotopic composition; Soil; Litter; Ashes; Combustion; Atmospheric emissions
Corresponding Author:	Anne Helene Helene Fostier, PhD State University of Campinas Campinas, BRAZIL
First Author:	Larissa Richter, PhD
Order of Authors:	Larissa Richter, PhD David Amouroux, PhD Emmanuel Tessier, PhD Anne Helene Helene Fostier, PhD
Abstract:	<p>Mercury (Hg) emissions from forest fires, especially tropical forests, contribute significantly to the atmospheric mercury budget. Recent studies have shown that the combustion process results in Hg isotope fractionation that allows tracking coal combustion Hg emissions. However, the potential of Hg stable isotopes to trace forest fire Hg emissions has never been investigated. Here we measured the Hg isotopic composition of litter, soil, and ash samples collected in prescribed forest fire experiments carried out in two localities of the Brazilian Amazonian Forest, Alta Floresta (AF) and Candeias do Jamari (CJ). For AF, where a small-scale experiment was performed, no difference was found in the mercury isotopic composition of the samples collected before and after burning. In contrast, the larger-scale experiment carried out in CJ resulted in significant mass dependent fractionation (MDF $\delta^{202}\text{Hg}$) in soils and ash. As for coal combustion, mass independent fractionation was not observed. This work highlights the potential of forest fires to cause Hg isotopic fractionation, depending on the fire severity. The results also allowed to establish an isotopic fingerprint for tropical forest fire Hg emissions that corresponds to a mixture of litter and soil Hg isotopic composition.</p>
Suggested Reviewers:	<p>Xuewu Fu Institute of Geochemistry Chinese Academy of Sciences fuxuewu@mail.gyig.ac.cn Dr. Xuewu Fu has high expertise on biogeochemical cycle study, working on atmospheric Hg emission and deposition processes, also using Hg isotopic composition in his studies</p> <p>Bridget Begquist University of Toronto bergquist@es.utoronto.ca Dr Begquist's research field concerns research on metal biogeochemistry (both laboratory and field) with studies of natural metal isotopic variations has the potential to yield insights into the modern global cycles of metals</p> <p>Jason Demers University of Michigan jdemers@umich.edu Dr Demers's research fields are Organometallic Chemistry, Environmental Chemistry and Geochemistry. Among others, he has skills and expertise on Mercury isotopes, Ecosystems, Environment, Forests, Streams, Atmospheric deposition, Biogeochemistry, Water Quality, Environmental Chemistry, Geochemistry</p> <p>Martin Jiskra University of Basel</p>

	<p>martin.jiskra@unibas.ch Dr Jiskra's field research concerns Mercury biogeochemical cycle, with many studies related to Hg emission/deposition in forest ecosystems and also using mercury isotopes in his investigations.</p>
	<p>Jean Remy Davee Guimaraes Federal University of Rio de Janeiro Carlos Chagas Filho Biophysics Institute jeanrdg@biof.ufrj.br Dr Guimaraes has been studying the mercury biogeochemical cycle in the Amazon for more than 30 years. He also has been using mercury isotopic composition in some of his studies.</p>
	<p>Ari Feinberg Massachusetts Institute of Technology arifein@mit.edu Dr Feinberg research focuses on atmospheric mercury (Hg) modelling. He recently published a paper highlighting the importance of vegetation uptake and deforestation in chemistry-transport model.</p>
<p>Opposed Reviewers:</p>	

Dear Editor of Chemosphere,

I am herewith enclosing the manuscript **“Impact of forest fire in the Amazon on the mercury stable isotopes composition in litter and soil”** to be considered for publication into the *Chemosphere Special Issue on “Environmental / Analytical Chemistry and/or Toxicology and Risk Assessments in Latin-American Countries”*.

Uptake of atmospheric Hg by forests, especially tropical forests, has been recognized to be the largest global mechanism for removal of atmospheric Hg. Conversely, forest fires increase direct emissions of mercury to air and remobilization of mercury stored in the terrestrial environment. Although Hg stable isotopes composition appears as a very performant tool to improve knowledge on different processes that make up the complex Hg biogeochemical cycle, its potential to trace forest fires Hg emissions has still not been investigated.

To fill this gap we measured the Hg isotopic composition of litter, soils and ashes samples collected in prescribed forest fire experiments carried out in two localities of the Brazilian Amazonian Forest. The work highlights the potential of forest fires to cause Hg isotopic fractionation depending on the fire severity. It also allowed to establish an isotopic fingerprint for tropical forest fires Hg emissions that corresponds to a mixture of litter and soils Hg isotopic composition.

As the Amazon rainforest accounts for more than half of the remaining tropical forests on the planet, we are convinced that this work makes an important contribution to a better understanding of the important processes involved in the Hg cycle in these ecosystems.

The authors certify that this is an original work that has not been previously published in a refereed journal, and it is not being submitted fully or partially for publication elsewhere. All the authors have read the manuscripts and agree with its publication.

Sincerely yours,

Anne H el ene Fostier
Environmental Chemistry Group
Institute of Chemistry
University of Campinas, Campinas, S ao Paulo, Brazil

- Hg isotopic composition of Amazon Forest soil, litter and ashes is measured
- Hg isotopic composition is determined before and after forest fire experiments
- Hg isotopes exhibit mass-dependent fractionation due to higher fire severity
- Hg isotopes show that forest fires emit soil and litter Hg to air and ashes
- Hg isotopic composition of tropical forest fire emissions is assessed

Larissa Richter: Conceptualization, Methodology, Investigation, Formal analysis, Writing – original draft.

David Amouroux : Conceptualization, Project administration, Writing-original draft, Writing-review and editing, Supervision.

Emmanuel Tessier: Investigation.

Anne Hélène Fostier: Conceptualization, Project administration, Writing-original draft, Writing-review and editing, Supervision.

Declaration of interests

The authors declare that they have no known competing financial interests or personal relationships that could have appeared to influence the work reported in this paper.

The authors declare the following financial interests/personal relationships which may be considered as potential competing interests:

Impact of forest fire on the mercury stable isotope composition in litter and soil in the Amazon

1 **Larissa Richter¹, David Amouroux^{2*}, Emmanuel Tessier², Anne H el ene Fostier^{1*}**

2 ¹ Institute of Chemistry, University of Campinas (UNICAMP), 13083-970, Campinas, S ao Paulo,
3 Brazil

4 ² Universit e de Pau et des Pays de l'Adour, E2S UPPA, CNRS, IPREM, Institut des Sciences
5 Analytiques et de Physico-chimie pour l'Environnement et les Mat eriaux, Pau, France;

6

7 *** Correspondence:**

8 david.amouroux@univ-pau.fr; annehfoitier@gmail.com

9 **Highlights:**

10 -Hg isotopic composition of Amazon forest soil, litter and ashes is measured

11 -Hg isotopic composition is determined before and after forest fire experiments

12 -Hg isotopes exhibit mass-dependent fractionation due to higher fire severity

13 -Hg isotopes show that forest fires emit soil and litter Hg to air and ashes

14 -Hg isotopic composition of tropical forest fire emissions is assessed

15

16

17

18

Graphical Abstract



23 **Abstract**

24 Mercury (Hg) emissions from forest fires, especially tropical forests, contribute significantly to the
25 atmospheric mercury budget. Recent studies have shown that the combustion process results in Hg
26 isotope fractionation that allows tracking coal combustion Hg emissions. However, the potential of Hg
27 stable isotopes to trace forest fire Hg emissions has never been investigated. Here we measured the Hg
28 isotopic composition of litter, soil, and ash samples collected in prescribed forest fire experiments
29 carried out in two localities of the Brazilian Amazonian Forest, Alta Floresta (AF) and Candeias do
30 Jamari (CJ). For AF, where a small-scale experiment was performed, no difference was found in the
31 mercury isotopic composition of the samples collected before and after burning. In contrast, the larger-
32 scale experiment carried out in CJ resulted in significant mass dependent fractionation (MDF $\delta^{202}\text{Hg}$)
33 in soils and ash. As for coal combustion, mass independent fractionation was not observed. This work
34 highlights the potential of forest fires to cause Hg isotopic fractionation, depending on the fire severity.
35 The results also allowed to establish an isotopic fingerprint for tropical forest fire Hg emissions that
36 corresponds to a mixture of litter and soil Hg isotopic composition.

37

38 **Keywords:** Mercury; Isotopic composition; Soil; Litter; Ashes; Combustion; Atmospheric emissions.

39

40 **Introduction**

41 Mercury (Hg) is a highly toxic and ubiquitous element in the environment (Outridge et al., 2018).
42 In the atmosphere, 90% to 99% is present as gaseous elemental mercury (GEM), with the remaining
43 portion composed of operationally-defined gaseous oxidized mercury (GOM) and particulate-bound
44 mercury (PBM) (Gustin et al., 2013). Foliage uptake has been shown to be an efficient process to
45 remove atmospheric GEM (Jiskra et al., 2018), but GOM and PBM can also be sorbed by or on leaves.
46 Mercury is then transferred to soil by litterfall and throughfall, where it accumulates. Forests have,
47 therefore, been recognized to play a key and global role in the biogeochemical cycle of this element
48 (Wang et al., 2016; Obrist et al., 2018; Zhou et al., 2021).

49 Due to their specificities such as high biomass productivity, leaf area index and leaf lifespan
50 (Witt et al., 2009), tropical and subtropical forests are especially efficient in removing atmospheric Hg
51 (Wang et al., 2016) and further storing it in soil (Wang et al., 2019). On the other hand, these forests
52 have also been submitted to intense rates of deforestation often associated with forest burning
53 (Carmenta et al., 2011). A number of studies have provided evidence that part of the Hg stored in
54 vegetation and soil is reemitted to the atmosphere during a forest fire (Friedli et al., 2009; Chen et al.,
55 2013; De Simone et al., 2015; Shi et al., 2019; Gworek et al., 2020), and it has been estimated that
56 43.3% of the total Hg budget emitted by forest burning can be attributed to tropical forests (Kumar et
57 al., 2018).

58 The Amazon rainforest accounts for over half of the planet's remaining tropical forest, and it
59 was estimated that it contributes to approximately 20% to 30% of the total Hg land sink (Fostier et al.,
60 2015; Feinberg et al., 2022). But, this biome also figures as an important Hg emitter due to enormous
61 annual deforestation (INPE, 2022). However, the Amazon remains a region with few studies focused
62 on this topic and with great uncertainties related to the emissions, thus increasing the difficulty in
63 establishing accurate mass balance and mathematical models to understand Hg fate during the burning
64 process in this region.

65 In recent years, studying Hg stable isotope composition appears as a very performant tool to
66 improve knowledge on different processes that make up the complex Hg biogeochemical cycle (Blum
67 et al., 2014; Bishop et al., 2020; Kwon et al., 2020). The basis of the technique is that Hg isotopes
68 undergo both mass dependent fractionation (MDF, reported as $\delta^{202}\text{Hg}$ (‰)) and mass independent
69 fractionation (odd-MIF, reported as $\Delta^{199}\text{Hg}$ (‰) and even-MIF, reported as $\Delta^{200}\text{Hg}$ (‰)) processes,
70 which enables investigation of possible Hg sources, its transformations and even fate in the
71 environment.

72 Many studies have been performed aiming to investigate mercury isotopic composition in
73 different types of forests (Demers et al., 2013; Zhang et al., 2013; Jiskra et al., 2015; Enrico et al.,
74 2016; Zheng et al., 2016; Wang et al., 2017; Liu et al., 2019), but only a few have focused on the
75 Amazon rainforest region (Fig. 1) (Araujo et al., 2018; Guedron et al., 2018; Miserendino et al., 2018;
76 Schudel et al., 2018). Furthermore, the potential of Hg stable isotopes to trace forest fire Hg emissions
77 has never been investigated.

78 In coal combustion processes, Sun et al. (2014) were the first to observe that GEM emitted from
79 coal-fire plants were enriched in heavier Hg isotopes, suggesting that isotopic fractionation may occur
80 during coal burning and fly ash removal processes. However, Li et al. (2021) observed that total
81 mercury emissions in flue gas from residential feed coal had similar isotopic composition than coal
82 itself, indicating that scale, temperature or other factors may influence isotopic fractionation during
83 burning, although many uncertainties still remain about this issue. As forest burning involves a
84 nonquantitative combustion process, it is expected to cause mercury isotopic fractionation.

85 The aim of this work was therefore to assess forest burning potential to cause mercury isotopic
86 fractionation (MDF and MIF) in different soil compartments (litter, soils and remaining ashes). The
87 study was performed in the Amazon rainforest in small- and larger-scale prescribed burning
88 experiments to assess some factors that can influence such isotopic fractionation.

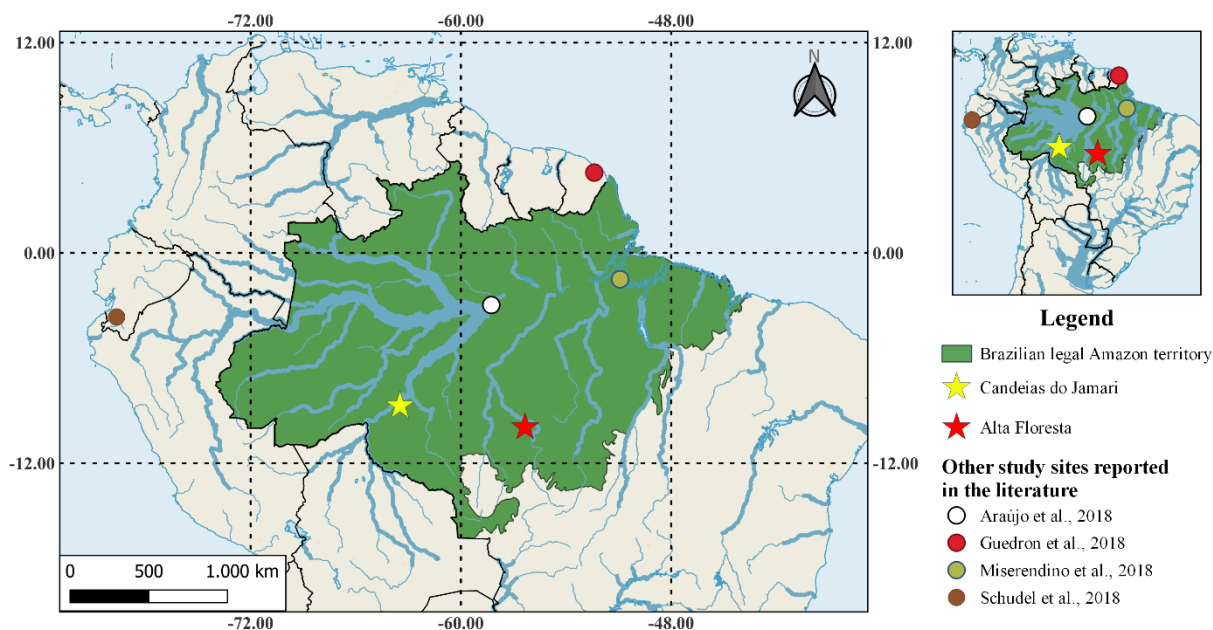
89

90 2. Materials and methods

91 2.1 Fire experiments and sampling

92 Fire experiments were carried out in two places (Fig. 1): Alta Floresta (AF) (9°56'40S,
93 56°19'48"W) and Candeias do Jamari (CJ) (8°45'1"S, 63°27'20"W). Both localities are in the so-
94 called *arc of deforestation*, a vast region with high rates of fire-based deforestation resulting from
95 efforts to transform forests in crop land (Carvalho et al., 2001). The vegetation type from the
96 experimental areas is old-growth *terra firme* forest (Chave et al., 2010) and the soils are leached
97 ferralitic soils, oxisols (Lacerda et al., 2004; Almeida et al., 2005). The climate of the region is humid
98 tropical, type Aw in the Koppen classification (Ferraz et al., 2005). The annual rainfall rate is around
99 2200 mm year⁻¹, with the rainy season lasting from November to April (Brown et al., 1995;
100 Aparecido et al., 2020).

101 At AF, six burning sub-area 2 × 2 m² plots of land were delimited inside the forest and a variable
102 amount of fuel (litter and branches) was placed within each experimental sub-area. Fuel material was
103 weighed before burning, and the remaining ash was weighed after burning to calculate biomass
104 consumption completeness (BCC (% m m⁻¹) according to equation S1 (Text S1) in Supplementary
105 Information (SI); detailed data on fuel loading and ash mass are also available in SI, Table S1. In these
106 experiments litter, soils and ashes were collected in each sub-area. Soil sampling was carried out to
107 depths of 0-1 cm and 1-2 cm before and after burning.



108

109 **Figure 1** - Map of the Brazilian legal Amazon territory, location of the study areas (Candeias do Jamari
 110 and Alta Floresta) and other works reported in the literature including Hg isotopes data for the
 111 Amazonian region (Araujo et al., 2018; Guedron et al., 2018; Miserendino et al., 2018; Schudel et al.,
 112 2018)

113 At CJ, a prescribed fire experiment was conducted in a $150 \times 150 \text{ m}^2$ plot (Fire experiment
 114 authorization 204/2014 Secretaria de Estado do Desenvolvimento Ambiental do Rondônia). Details on
 115 this experiment are given in the SI (Text S2). Briefly: the forest was cleared at the beginning of the dry
 116 season (June-August) and burned in August. BCC was estimated according to equation S1 (SI, Text
 117 S1) through the results obtained for nine different $2 \times 2 \text{ m}^2$ sub-area plots in which litter, soil (0-1, 1-
 118 2, 2-5 cm) and ash were sampled. It is important to notice, that at both sites, after burning the 0-1-cm
 119 layer visually corresponded to the burned O-horizon, and ash mainly to the burned biomass. Details on
 120 fuel loading, ash mass and BCC on each sub-area are presented in SI, Table S2.

121 In both experiments, soil and ash sampling were performed according to the method described
 122 by Melendez-Perez et al. (2014). The samples were dried at room temperature on laminar flow hood,
 123 milled in mortar with liquid N_2 and stocked at room temperature in HDPE flasks.

124 2.2 Total Hg determination

125 Total mercury (Hg_{Tot}) determination was carried out by thermo-desorption atomic absorption
 126 spectrometry (DMA-80 Tri Cell, Milestone, Italy) according to Melendez-Perez and Fostier (2013).
 127 Accuracy was assessed in terms of recovery (%) by analyzing Standard Reference Materials and was
 128 $113 \pm 8\%$ for NIST 2689 (Trace elements in coal), $113 \pm 5\%$ for NIST 1632d (coal fly ash), $93 \pm 2\%$
 129 for IAEA 336 (lichen) and $99 \pm 5\%$ for IAEA 433 (marine sediment). Precision expressed as the
 130 relative standard deviation of three analytical repetitions was $<10\%$. Detection limit (DL) and
 131 quantification limit (QL) were 1.7 ± 0.1 and 5.6 ± 0.5 $ng\ g^{-1}$, respectively, for litter analyses, 1.3 ± 0.1
 132 $ng\ g^{-1}$ and 4.5 ± 0.4 $ng\ g^{-1}$ for ash, and 0.75 ± 0.06 and 2.5 ± 0.2 $ng\ g^{-1}$ for soil.

133

134 2.3 Isotopic composition analysis

135 For isotopic composition analysis, two sample preparation methods were used. In the first one,
 136 approximately 1000 mg of ash, litter or soil sample were digested with 5 mL HNO_3 and 0.5 mL H_2O_2
 137 in a high-pressure Asher (HPA-S, Anton Paar) according to Barre et al. (2018, 2020). For the second
 138 one, between 500-800 mg of sample were decomposed in 50 mL PP vial with 5 mL of $HNO/HCl/H_2O_2$
 139 (3:1:1, v:v:v) at 85 °C for 48 h, (Guedron et al., 2018). For soils, the first method was only used for
 140 more complex samples and those with lower Hg concentration.

141 Mercury isotope analyses were performed with a cold vapor generation system (CVG) with
 142 $SnCl_2$ reduction coupled to a multicollector (MC) – mass spectrometer with inductively coupled plasma
 143 (ICP-MS) (Nu Plasma, Nu Instrument) as described by Barre et al. (2020). MDF and MIF are expressed
 144 according to the equations recommended by Bergquist and Blum (2007) as follows in Eq. 1 and 2,
 145 respectively.

$$146 \quad \delta^{XXX}Hg\ (\%) = \left[\left(\frac{^{XXX}Hg}{^{198}Hg} \right)_{sample} / \left(\frac{^{XXX}Hg}{^{198}Hg} \right)_{CRM\ NIST\ 3133} - 1 \right] * 1000 \quad (1)$$

$$147 \quad \Delta^{XXX}Hg = \delta^{XXX}Hg - (\beta_{XXX} \cdot \delta^{202}Hg) \quad (2)$$

148 Where xxx corresponds to the studied isotope in the sample and in the CRM NIST 3133
149 solution, monitored following a standard bracketing method as a Hg isotopic composition reference in
150 the same concentration as the sample (1.0, 0.5 and 0.25 $\mu\text{g L}^{-1}$); and β_{xxx} is the kinetic mass-
151 dependence scale factor, characteristic of each isotope mass (for ^{199}Hg is 0.2520, ^{200}Hg 0.5024, ^{201}Hg
152 0.7520 and for ^{204}Hg 1.493). The instrumental mass-bias was corrected by using the internal standard
153 of Tl (NIST 997, $^{205}\text{Tl}/^{203}\text{Tl} = 2.38714$). NIST 8610 (former UM-Almadén) standard solution was
154 monitored during each analytical session as a quality control of the isotopic composition analyses.
155 Multiple measurements of the certified reference materials (CRM) BCR-482 (lichen), IAEA 336
156 (lichen) and IAEA 405 (marine sediment) were also performed. The consistency between the average
157 isotopic composition of each material obtained in the present study and those previously published in
158 the literature (Table S3) attests to the good accuracy of the method. The precision method, expressed
159 as 2 standard deviations of the N measurements, is also given in Table S3.

160 For litter, ash, and soil samples, recovery (R%) was estimated as the total Hg concentration
161 measured by CVG/MC-ICP-MS*100/total Hg concentration measured by TD-AAS. The precision
162 measurement (expressed as 2SD for CVG/MC-ICP-MS analyses) was calculated from three analytical
163 replicates. When considering all the analyzed samples, average recovery was $96 \pm 11\%$, $99 \pm 7\%$ and
164 $90 \pm 8\%$ for litter, ash, and soils respectively, and for $\delta^{202}\text{Hg}$, $\delta^{200}\text{Hg}$, $\Delta^{200}\text{Hg}$ and $\Delta^{201}\text{Hg}$, 2SD was
165 $<0.15\%$.

166 Uncertainties of the isotopic composition measurements were defined as follows: when the
167 measurement precision of CRM NIST 8610 for a particular isotope was greater than the obtained value
168 for a particular type of sample, the values of 2SD of NIST 8610 were considered, as observed for litter
169 and soil samples; when a particular type of sample presented greater values of 2SD than NIST 8610,
170 the samples 2SD were considered, as observed for ash samples.

171

172 2.4 Complementary analyses

173 The organic matter content was obtained by gravimetric method after calcination for 2 h at 360
174 °C (North Central Regional Research, 2012). Elemental composition (C, H, N) was determined with
175 an elemental analyzer (PerkinElmer, 2400 System, Waltham, MA, US).

176 2.5 Statistical data treatment

177 Different data treatments were performed using Origin 8.1[®], Microsoft Excel[®] and Xlstat[®]
178 software. All the results were assessed for normal distribution using the Shapiro-Wilk test ($\alpha=5\%$).
179 When the results were not normally distributed, nonparametric statistical tools (Kruskal Wallis test
180 combined with Conover-Iman with Bonferroni correction) were used to compare the data to each other.

181

182 3. Results

183

184 3.2 Total Hg concentration in litter, ash, and soil

185 Concentration of Hg_{Tot} in all analyzed samples are given in Table 1 (detailed data in Table S4
186 and S5). For litter, Hg_{Tot} at AF ($54 \pm 9 \text{ ng g}^{-1}$) was significantly higher ($p = 0.002$) than at CJ (33 ± 8
187 ng g^{-1}). In wood, Hg_{Tot} were $8.8 \pm 1.1 \text{ ng g}^{-1}$ and $< \text{LQ}$ (1.3 ng g^{-1}) for the samples from AF and CJ,
188 respectively. In ash, Hg_{Tot} was in the same range (12 to 31 ng g^{-1}) in AF and CJ samples. In both sites
189 the concentrations in ash were lower than in litter ($p = 0.01$ for AF and $p = 0.03$ for CJ). In AF soil,
190 Hg_{Tot} significantly decreased after burning for both depths (0-1 cm: $p = 0.02$ and 1-2 cm: $p = 0.03$),
191 while at CJ significant decreases were only observed for the surface layer (0-1 cm: $p = 0.02$).

192

193

194 **Table 1.** Total mercury concentration (ng g⁻¹) in litterfall, ash and soil samples collected before (BB)
 195 and after (AB) burning at Alta Floresta (AF) and Candeia do Jamari (CJ) experimental sites.

		Litter	Ash	Soil					
				0-1 cm		1-2 cm		2-5 cm	
				BB	AF	BB	AF	BB	AF
AF	N ^(a)	5	5	6	6	6	6	-	-
	Range	40 – 65	13 - 31	68 - 93	57 - 77	67 - 82	60 - 79	-	-
	Mean ± SD ^(b)	54 ± 9	23 ± 6	79 ± 9	66 ± 7	75 ± 6	69 ± 8	-	-
	Median	55	23	81	67	76	68	-	-
CJ	N ^(a)	9	9	9	9	9	9	9	9
	Range	25 – 50	12 - 31	135 - 172	113 - 167	136 - 172	126 - 169	138 - 167	131 - 168
	Mean ± SD ^(b)	33 ± 8	23 ± 8	148 ± 13	134 ± 21	148 ± 12	146 ± 16	150 ± 12	151 ± 13
	Median	33	24	144	125	146	141	149	151

196 (a) N: number of samples; (b) SD: standard deviation

197

198 3.2 Hg isotopic composition in soil, litter and ash

199 Averages of the isotopic composition and main results per type of sample and locality are
 200 given in Table 2. Complete data of Hg isotopic composition from samples are given in
 201 Supplementary Information (Table S6 and S7), while probabilities for each comparison between
 202 different datasets are given in Table S8.

203

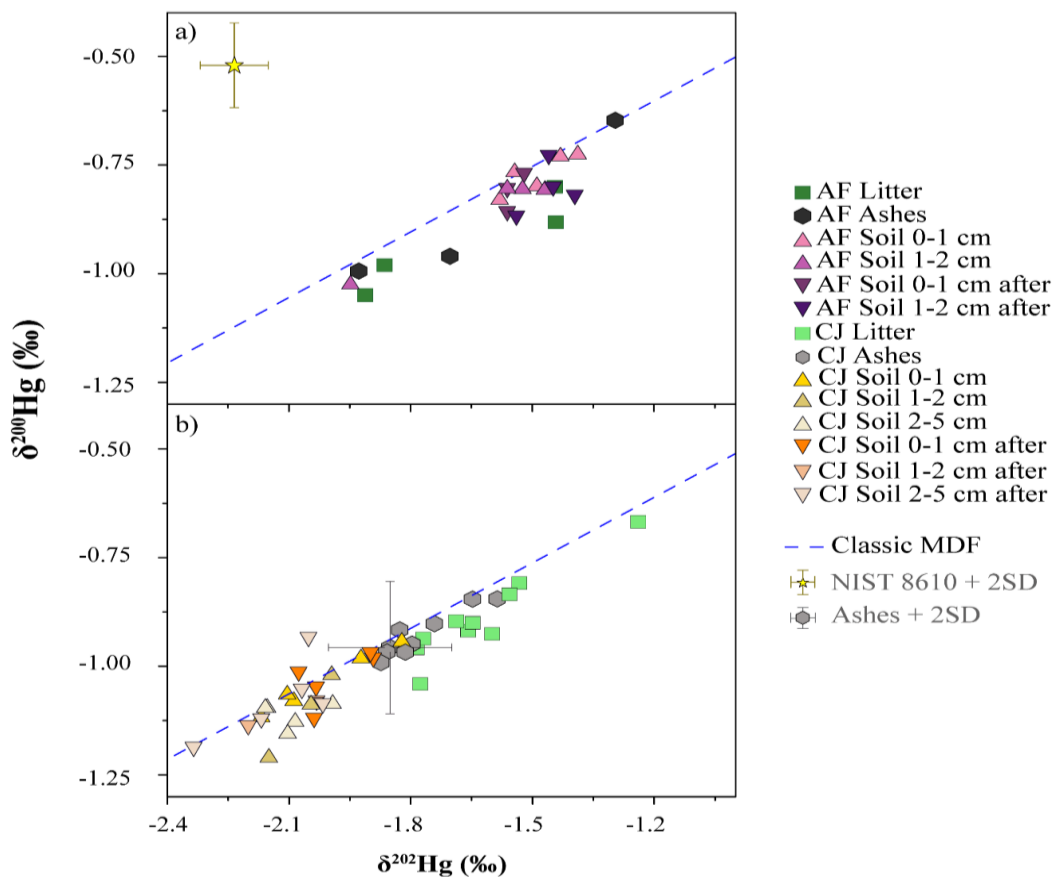
204 **Table 2.** Main results of the Hg isotopic composition per type of sample and locality

Locality	Type of sample	N ^(a)		$\delta^{202}\text{Hg}$	$\delta^{200}\text{Hg}$	$\Delta^{200}\text{Hg}$	$\Delta^{199}\text{Hg}$	
				(‰)	(‰)	(‰)	(‰)	
Alta Floresta	Litter	4	Mean	-1.66	-0.93	-0.09	-0.54	
			SD	0.26	0.11	0.05	0.07	
	Ash	3	Mean	-1.64	-0.87	-0.04	-0.56	
			SD	0.32	0.19	0.06	0.02	
	Soils before burning	8	Mean	-1.56	-0.82	-0.03	-0.52	
			SD	0.17	0.09	0.02	0.07	
		Soils after burning	7	Mean	-1.50	-0.81	-0.06	-0.53
				SD	0.06	0.05	0.05	0.04
	Litter	10	Mean	-1.62	-0.89	-0.07	-0.36	
			SD	0.17	0.11	0.04	0.06	
	Candeias do Jamari	Ash	9	Mean	-1.78	-0.93	-0.03	-0.58
				SD	0.10	0.05	0.02	0.06
Soils before burning		12	Mean	-2.05	-1.07	-0.04	-0.59	
			SD	0.10	0.07	0.04	0.03	
Soils after burning		13	Mean	-2.08	-1.07	-0.03	-0.63	
			SD	0.12	0.08	0.05	0.03	

(a): N, number of analyzed samples

206 *Mass dependent fractionation*

207 Regarding $\delta^{202}\text{Hg}$ in AF (Fig. 2a, Table 2), no significant difference ($p>0.05$, Table S8) was
 208 observed between litter, soil and ash, before and after burning. In contrast, in CJ (Fig. 2b) significant
 209 differences ($p<0.05$) were observed between 1) litter and soil before burning, 2) litter and soil after
 210 burning, 3) ash and soil before burning, and 4) ash and soil after burning. Comparing the results from
 211 AF and CJ, no significant difference was observed between $\delta^{202}\text{Hg}$ of litter and ash from both sites
 212 ($p=0.94$ for litter and $p=0.47$ for ash). For soils, however, significant differences were obtained
 213 between AF and CJ ($p<0.05$ before/after burning).



214

215 **Figure 2.** Graph of $\delta^{200}\text{Hg}$ versus $\delta^{202}\text{Hg}$ for litter, ash and soil samples from a) Alta Floresta (AF)
 216 and b) Candeias do Jamari (CJ). Soil samples are divided into different depths (0-1, 1-2 or 2-5 cm)
 217 and before or after (aft.) fires. * For the CRM NIST 8610, IC is represented in another range of the
 218 graph, and results are inserted at the top of the graph just to represent the magnitude of the
 219 uncertainty of the validated methods.

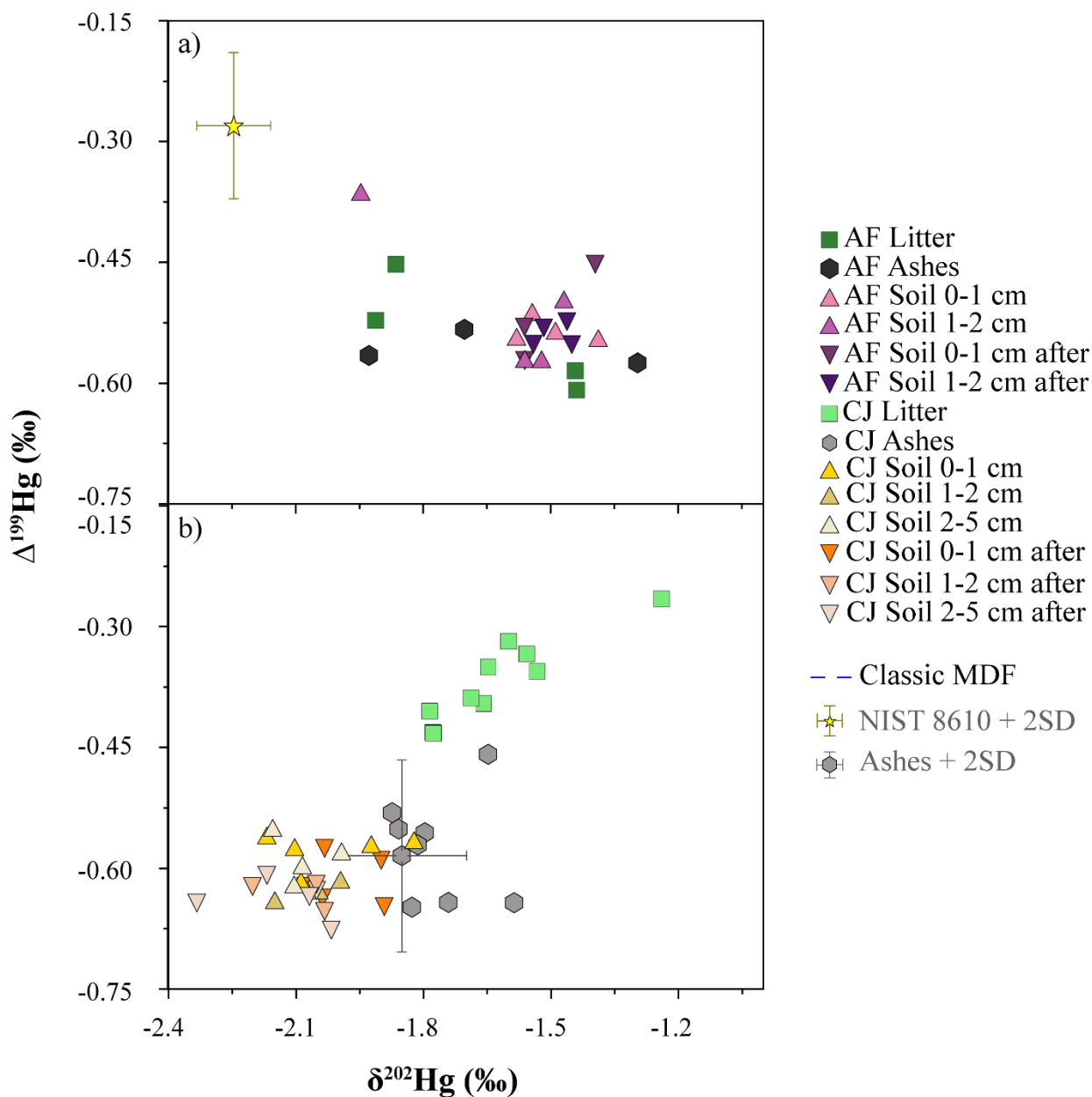
220

221 *Odd and even mass independent fractionation*

222 Variations of Hg $\delta^{200}\text{Hg}$ and $\delta^{199}\text{Hg}$ as a function of $\delta^{202}\text{Hg}$, respectively presented on Fig. 2
223 and Fig. S1, allow to assess if both odd and even Hg isotopes follow a strictly MDF process or exhibit
224 significant deviation inherent to Hg isotopes MIF. The $\delta^{200}\text{Hg}/\delta^{202}\text{Hg}$ ratio of all AF (Fig. 2a) and CJ
225 (Fig. 2b) samples clearly follows a linear distribution with the same slope as expected for Hg isotopes
226 MDF (Blum et al., 2014), suggesting no even Hg isotopes MIF. This observation is clearly validated
227 in Fig. S2 ($\Delta^{200}\text{Hg}$ compared to $\delta^{202}\text{Hg}$) and Fig. S3 ($\Delta^{200}\text{Hg}$ compared to $\Delta^{204}\text{Hg}$), that explicitly
228 illustrate that $\Delta^{200}\text{Hg}$ and $\Delta^{204}\text{Hg}$ extent and variations are not significant between the localities and
229 samples (i.e. considering analytical precision). The variation of $\delta^{199}\text{Hg}$ as a function of $\delta^{202}\text{Hg}$ (Fig.
230 S1) roughly follow the classical MDF line. However, for CJ (Fig. S1b), litter presented significant
231 deviations from the MDF line, suggesting that MIF-odd is statistically significant. Odd MIF extents
232 for Hg isotopes are indeed different from zero and exhibit negative average values as shown in Table
233 2. Variation of odd-MIF for Hg isotopes is highlighted by Fig. S2 showing $\Delta^{199}\text{Hg}$ compared with
234 $\Delta^{201}\text{Hg}$ plot, in which a clear difference appears between CJ litter and other samples from both localities
235 ($p < 0.05$, Table S8).

236 Figure 3 represents odd-MIF compared with MDF of Hg isotopes ($\Delta^{199}\text{Hg} \times \delta^{202}\text{Hg}$). It shows
237 that for AF (Fig. 3a) the obtained isotopic composition of the different types of samples mainly overlap
238 and no discrimination of specific sample types can be verified. However, for CJ (Fig. 3b), litter samples
239 are separated from the others due to their enrichment in $\Delta^{199}\text{Hg}$ when compared with other samples
240 (ash and soil) from the same location ($\epsilon(\Delta^{199}\text{Hg}) \sim 0.15\%$, $p < 0.05$). Ashes compared to soils are in the
241 same odd-MIF range ($\Delta^{199}\text{Hg}$), while they present an enrichment (ϵ) in $\delta^{202}\text{Hg}$ of about $+0.2\%$.

242



243

244 **Figure 3.** Graphic of $\Delta^{199}\text{Hg}$ compared with $\delta^{202}\text{Hg}$ for litter, ash and soil samples from a) Alta
 245 Floresta (AF) b) Candeias do Jamari (CJ). Soil samples are divided into different depths (0-1, 1-2 or
 246 2-5 cm) and before or after (aft.) fires.* For the CRM NIST 8610, IC is represented in another range
 247 of the graph, and results are inserted at the top of the graph just to represent the magnitude of the
 248 uncertainty of the validated methods.

249 4. Discussion

250

251 4.1 Mercury distribution and its isotopic composition as a function of sample type and burning 252 experiment

253

254 **Litter:** Total Hg concentration in litter from AF and CJ significantly differed (Table 1), which could
255 be related to the different operational approach used in each experiment. The clearing of the forest at
256 the beginning of the dry season in CJ left the litter exposed to solar radiation (i.e. UV-visible light and
257 heat) and rain washout for several months. These conditions could have respectively promoted direct
258 atmospheric evasion and leaching of Hg from exposed litter, and therefore, reduced the total Hg content
259 in litter at this site. In contrast, the AF experiment was carried out under forest cover, below the canopy,
260 preventing litter from being frequently exposed to intense solar radiation or rain washout, and
261 consequently reduced potential Hg loss from the litter. This hypothesis is confirmed by the Hg_{Tot}
262 ($57 \pm 3 \text{ ng g}^{-1}$) of an additional litter sample collected inside the forest at CJ, which is much closer to
263 the concentration obtained in AF and to the average concentration reported for litter in the Amazon
264 forest (Fostier et al., 2015).

265 Despite these conclusions, the differences between the isotopic composition in litter from AF
266 and CJ cannot only be explained by potential photochemical induced reduction and volatilization of
267 Hg. Although such a process could generate significant MDF and odd-MIF of the Hg isotopes, the litter
268 sample collected under the forest canopy of CJ exhibits very similar isotopic composition to the litter
269 samples from the burning experiment area (Table 2). This suggests that the differences in litter Hg
270 concentration and isotopic composition between CJ and AF are mainly caused by non-photochemical
271 solar heating and/or rain washout processes for which only MDF and negligible MIF of the Hg isotopes
272 are expected (Blum et al., 2014). However we do not have data regarding isotopic fractions for such

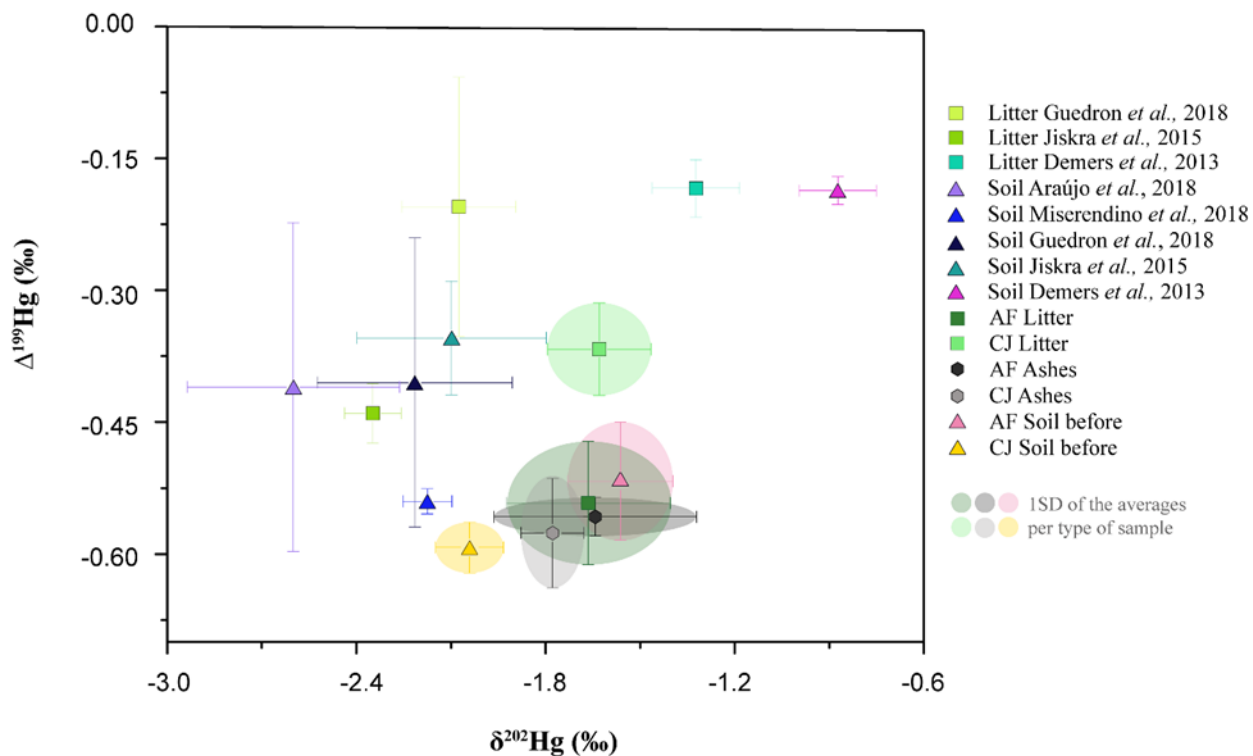
273 specific pathways, and differences measured for both concentration and isotopic composition could
274 also be attributed to specific regional and ecological differences between both locations such as
275 atmospheric total gaseous Hg, predominant plant species, tree and leaf age, among other factors (Yuan
276 et al., 2019).

277 The greater differences between the isotopic composition for litter from different localities
278 appear for MDF (Fig. 4). In temperate forest system, Demers et al. (2013) obtained a MDF extent for
279 litter of $\delta^{202}\text{Hg} = -1.32 \pm 0.14\text{‰}$, which is markedly higher than the present study. Meanwhile, more
280 negative MDF values were reported in another tropical rainforest (Guedron et al. (2018): $\delta^{202}\text{Hg} = -$
281 $2.01 \pm 0.18\text{‰}$) and a boreal forest (Jiskra et al. (2015): $\delta^{202}\text{Hg} = -2.35 \pm 0.09\text{‰}$). These large
282 differences can be related to many factors such as atmospheric Hg_{Tot} , tree species and tree and leaf age
283 that result in different uptake of atmospheric Hg (Zhou et al., 2021). The large $\delta^{202}\text{Hg}$ extent ($\sim 1.0\text{‰}$)
284 suggests that the type of forest doesnot have a clear influence on Hg MDF isotopic composition in
285 litter.

286 For odd-MIF in litter from tropical forest, Guedron et al. (2018) obtained $\Delta^{199}\text{Hg} = -$
287 $0.20 \pm 0.15\text{‰}$, values that are less negative than those obtained in the present study. This can be
288 explained because those samples were collected close to a former gold mining site. Indeed, metallic
289 Hg commonly used in small-scale gold mining has an odd-MIF close to zero. In Demers et al. (2013),
290 odd MIF average was higher ($\Delta^{199}\text{Hg} = -0.18 \pm 0.03\text{‰}$, but most likely reflects the isotopic composition
291 of atmospheric Hg in a region largely influenced by industrial anthropogenic inputs. In Jiskra et al.
292 (2015), odd-MIF average ($\Delta^{199}\text{Hg} = -0.44 \pm 0.03\text{‰}$) is similar to our study.

293 Nonetheless, results of $\delta^{202}\text{Hg}$, $\Delta^{199}\text{Hg}$ and $\Delta^{200}\text{Hg}$ in litter indicate that the origin of Hg in these
294 samples is mostly atmospheric, as demonstrated in previous investigations, and exhibits negative MDF,
295 slightly negative odd-MIF and close to zero even-MIF (Demers et al., 2013; Jiskra et al., 2015; Araujo

296 et al., 2018; Guedron et al., 2018; Miserendino et al., 2018; Yuan et al., 2019; Barre et al., 2020; Wang
 297 et al., 2021; Zhou et al., 2021).



298
 299 **Figure 4.** Graphic of $\Delta^{199}\text{Hg}$ as a function of average $\delta^{202}\text{Hg}$ for litter, ash and soil samples analyzed
 300 in this work compared to other forest samples reported in the literature. Sources: Araujo et al. (2018),
 301 Demers et al. (2013), Guedron et al. (2018), Jiskra et al. (2018) and Miserendino et al. (2018).

302
 303 **Soil:** The average concentrations of Hg_{Tot} in soils of both study sites before burning (Table 1) are in
 304 the same range as those previously reported in the literature (e.g. Lacerda et al. (2004) and Michelazzo
 305 et al. (2010) for AF, and Almeida et al. (2005) for CJ). At both sites, Hg_{Tot} before burning was
 306 homogeneously distributed in the different soil layers.

307 At AF, both the organic layer (0-1 cm) as the mineral layer (1-2 cm) had significant mercury
 308 losses after burning, with $16 \pm 12\%$ of the mercury budget lost in the first layer and $6 \pm 5\%$ in the
 309 second layer. Conversely, at CJ only the organic layer (0-1 cm) had significant losses ($13 \pm 8\%$) (Table

310 S5), indicating that even though at CJ the burning experiment was much more severe than in AF (as
311 discussed in section 4.3), mercury emissions from soils may be affected by several parameters.

312 Regarding the isotopic composition, large differences for MDF ($\delta^{202}\text{Hg}$) were observed
313 between AF and CJ. Hg isotopic composition in soils may vary widely depending on the geogenic Hg
314 contribution, origin of the atmospheric Hg deposition, type of soil and even how the nutrient cycling
315 occurs at each location (Blum et al., 2014; Zheng et al., 2016), as illustrated in Fig. 4 reporting data
316 from different forested ecosystems. For North American temperate forests not directly impacted by
317 anthropogenic sources, the MDF and MIF-odd values reported by Demers et al. (2013), ($\delta^{202}\text{Hg} = -$
318 $0.87 \pm 0.12\text{‰}$; $\Delta^{199}\text{Hg} = -0.19 \pm 0.02\text{‰}$) are very different from those obtained in this study.
319 Conversely, the values reported by Araujo et al. (2018) ($\delta^{202}\text{Hg} = -2.60 \pm 0.34\text{‰}$; $\Delta^{199}\text{Hg} = -$
320 $0.38 \pm 0.22\text{‰}$) and Miserendino et al. (2018) ($\delta^{202}\text{Hg} = -2.12$ to $-2.23 \pm 0.14\text{‰}$; $\Delta^{199}\text{Hg} = -0.55\text{‰}$) who
321 also assessed nonimpacted forests in the Amazon, are closer to those obtained in our study. Among the
322 forests, systematic negative values of MDF and MIF falling in a close range confirm the importance
323 of all forests for the scavenging of atmospheric gaseous Hg and the litterfall transfer of this Hg from
324 the litter to the soil.

325 The Hg isotopic composition does not exhibit significant differences in the soils sampled before
326 and after burning, except for $\Delta^{199}\text{Hg}$ from CJ (Table S8). These results may indicate that although fire
327 leads to quantifiable Hg emissions from soil, this does not necessarily result in a significant isotopic
328 fractionation of the residual fraction remaining in the soil.

329 **Ash:** The presence of Hg in ash after the burning experiments may be attributed to the incomplete
330 emission of Hg initially present in the litter, and to the uptake of Hg emitted from the surface soil
331 during burning. Despite some differences observed in the Hg_{Tot} and Hg isotopic composition of the
332 litter and soil samples, ash from AF and CJ presented similar Hg_{Tot} (Table 1) and similar isotopic
333 composition ($p > 0.05$ for Hg_{Tot} and Hg isotopes, Table S8). This can be related to the similarities in the

334 chemical composition of the ash from both locations. Ash chemical composition did not differ
335 significantly ($p>0.05$) between both sites for organic matter (Table S4), Hg_{Tot} and major element
336 composition (C, H, N) (Table S9). This suggests that Hg content and Hg isotopic composition in ashes
337 can be significantly constrained by the ash chemical characteristics, that can vary under different
338 burning experimental conditions. Therefore, the influence of the final ash composition, and the Hg
339 fractionation confirm that Hg uptake by ashes is closely related to re-adsorption or condensation
340 mechanisms of Hg onto ash particles during and after the burning experiment. This hypothesis can
341 explain the final Hg isotopic composition of the ash, but not the exact main source of this Hg in the
342 cleared forest system.

343 According to Sun (2019) who reviewed Hg isotopic fractionation associated with the coal
344 combustion process, if MDF processes are expected during coal combustion, MIF are not. Reviewed
345 literature data mainly reports enrichments in heavier isotopes in ash material, following MDF law,
346 when compared to coal Hg isotopic composition. Using the same assumption for forest fires, the
347 differences measured in MIF extent between litter and ash at CJ (Fig. 3b) suggests that the litter
348 contribution to the Hg recovered in ash was low or insignificant. Indeed, for CJ, $\Delta^{199}Hg$ determined in
349 ash was significantly lower than in litter ($\Delta^{199}Hg$ litter = $-0.37 \pm 0.05\text{‰}$; $\Delta^{199}Hg$ ash = $-0.58 \pm 0.07\text{‰}$).
350 Conversely, $\Delta^{199}Hg$ in ash was like that in soils before burning ($\Delta^{199}Hg$ ash = $-0.59 \pm 0.03\text{‰}$),
351 suggesting that Hg in ash mainly originated from soils. In addition, $\delta^{202}Hg$ in ash at CJ was
352 significantly higher than in soils before burning (Fig. 2b). This suggests that an MDF process occurs
353 during soil heating and burning. This can be explained by the emission of lighter Hg isotopes to the
354 atmosphere and a simultaneous ash enrichment of heavier Hg with higher $\delta^{202}Hg$. This corroborates
355 the fact that forest fire can follow similar basic processes than coal combustion in a power plant as
356 reported by Sun (2019).

357 The fractionation of Hg and the associated isotopic composition can likely be explained by the
358 equilibrium between the two main Hg species emitted during a combustion process, such as GEM and
359 particular bound Mmercury (PBM). When Hg is emitted during biomass combustion, both species are
360 occurring, but their proportion can vary according to moisture and fuel nature, among other factors
361 (Obrist et al., 2018). Furthermore, PBM is more easily deposited after burning than GEM and can
362 easily be adsorbed on ash (De Simone et al., 2017; Sun, 2019). For coal combustion, Sun et al. (2014)
363 reported significant isotopic fractionation following MDF pathways. They determined higher $\delta^{202}\text{Hg}$
364 in the PBM associated with ash material, which was then enriched in heavier isotopes compared to
365 GEM Hg isotopic composition. This resulting ion is very similar to our observation for ash isotopic
366 composition at the CJ location. However, such an increase of $\delta^{202}\text{Hg}$ in ash was not observed during
367 the AF experiment, which indicates that other parameters are involved in the Hg fractionation processes
368 from soils and that significant MDF of Hg stable isotopes will not necessarily occur in all fires.

369

370 **4.3 Factors influencing Hg isotopic composition during forest fire**

371 Although the present dataset provided some information on Hg isotopic fractionation during
372 forest fires, it also highlights how fractionation processes can vary according to the type of forest fire,
373 especially for soil emissions.

374 One of the factors that differentiates forest fires is the severity, which is related to the intensity
375 of burning and depends on factors that govern the fire behavior (e.g. propagation rate, duration and
376 height of the flames), climatic conditions (temperature, relative humidity, wind and rain), topography,
377 and quantity, size and moisture of live and dead vegetal fuel and its chemical and structural composition
378 (Keeley et al., 2009; Mataix-Solera et al., 2011; Abraham et al., 2018). Although measuring burning
379 severity is still a challenge due to the many variables involved, some parameters are frequently used to
380 this end (Engle et al., 2006; Keeley et al., 2009).

381 In the experiments of AF and CJ, the consumption of biomass and the variations of organic
382 matter content in soil were used to assess the burning severity. Biomass consumption completeness at
383 AF averaged $80 \pm 10\%$, while at CJ it was 90 ± 11 (Table S1 and S2). For the soil organic matter content
384 [OM, % w w⁻¹], different behaviors were observed between both locations (Table S10). In AF, [OM]
385 did not change significantly after burning ([OM]_{0-1 cm} before = $18 \pm 6\%$; [OM]_{0-1 cm} after = $16 \pm 5\%$; p =
386 0.55), while in CJ this variation was substantial ([OM]_{0-1 cm} before = $21 \pm 5\%$; [OM]_{0-1 cm} after
387 = $14 \pm 4\%$; p = 0.005). This indicates that burning at CJ resulted in an important consumption of soil
388 organic matter, likely due to longer combustion and higher temperatures (Merino et al., 2018). Thus,
389 we hypothesize that the burning conditions at CJ allowed higher temperatures to be reached during the
390 experimental fire, enabling the consumption of the soil organic matter and the emission and isotopic
391 fractionation of Hg between soils and ashes.

392 Likewise, different parameters influencing the severity of burning in previous studies were
393 found to modify the isotopic composition of other elements, such as carbon, oxygen and nitrogen (Kato
394 et al., 1999; Schumacher et al., 2011). Kato et al. (1999) observed that during biomass burning
395 processes the volatile carbon species formed during the initial flaming phase were enriched in
396 isotopically heavier carbon species (¹³C enrichment) compared to the initial fuel material, which
397 exhibited lighter carbon isotopic composition (¹³C depletion) throughout the burning process and
398 during the smoldering phase (i.e. flameless burning phase with significant gas emissions). Therefore,
399 different burning settings that can result in a longer or smaller smoldering phase may influence
400 differently the isotopic composition of the burning products, favoring either the production of
401 isotopically lighter or heavier species. Based on the same assumptions for Hg emissions from soils
402 during biomass burning, more pronounced isotopic fractionations (i.e. MDF) may be expected in longer
403 burning episodes with more pronounced smoldering phases. These conditions in which greater amount
404 of energy is given throughout a longer burning period were likely achieved during CJ experiment.

405 Schumacher et al. (2011) evaluated the oxygen isotopic composition (^{16}O vs ^{18}O) in the CO_2
406 formed after the combustion of different types of fuels and under different conditions. They reported
407 that the composition of the fuel load and the comburent gases strongly influence the isotopic
408 composition of the emitted CO_2 . However, several processes may affect whether the resulting gas will
409 have an isotopic composition either more relatable to the comburent gas (i.e. lighter isotopic
410 composition or ^{16}O enrichment), or to the fuel load (plant tissues, with heavier isotopic composition
411 for carbon and oxygen). For wet fuel samples, the fractionation was smaller, resulting in lighter isotopic
412 composition (depletion of ^{13}C and ^{18}O isotopes) of the CO_2 compared with dry fuels. These authors
413 also observed that for higher temperatures reached during burning, the gases produced had heavier
414 carbon and oxygen isotopic composition compared to smaller temperatures, indicating that when
415 higher temperatures are reached the influence of the fuel isotopic composition may increase in the final
416 product.

417 Expanding these previous conclusions for lighter elements to Hg emissions during biomass
418 burning, several parameters may affect Hg fractionation and isotopic composition during forest burning
419 episodes. Even though the temperature was not measured during the burning experiments, we suggest
420 that the combustion temperature and fuel moisture may act as important factors for Hg emission and
421 fractionation in the soil/litter/ash system. These hypotheses are based on the fact that no significant
422 losses of soil OM were observed for AF experiment with dominant wet fuels, while much drier fuels
423 were burnt during the CJ experiment. During burning, OM consumption can only be observed above
424 $300\text{ }^\circ\text{C}$ (González-Pérez et al., 2004) and fuel moisture directly impacts the combustion completeness
425 and therefore, the fire temperature itself (Certini, 2005). This infers that these two factors are both
426 significantly influencing differences in the fate and fractionation of Hg observed between AF and CJ
427 experiments.

428 Considering the isotopic composition of the fuel material (i.e. litter and surface soils) and of
429 the resulting ash and soil after burning, we suggest that Hg from the litter was almost totally emitted

430 to the atmosphere while Hg from surface soil was partially and variably emitted as a function of several
431 parameters, such as fire temperature and moisture content of fuel. We highlight here that the burning
432 conditions play a fundamental role in the isotopic fractionation of the Hg species emitted, suggesting
433 that further controlled experiments are required to better understand this complex dynamic.

434

435 **4.4 Mercury isotopic fingerprint of forest fire emissions**

436 Rayleigh's equation is commonly used to access the isotopic composition during a particular
437 chemical reaction. It describes the partition between two isotopes as the initial reservoir decrease along
438 with reaction advancement and time. This equation can only be used if the following principles are
439 applied: 1) the material is continually removed from a mixed system that contains all the evolved
440 species; 2) The isotopic fractionation can be described in any instant by a fractionation factor (α) and
441 3) α does not change throughout the process (Kendall and Doctor, 2003; Hintelmann and Zheng, 2011).

442 As pointed out in the previous discussion, several variables act simultaneously during forest
443 burning, making it almost impossible to determine a fractionation factor for such complex processes
444 and environments. A conservative approach may be applied to provide an initial estimate of the forest
445 burning Hg isotopic signature emitted to the atmosphere. Considering the evolved environmental
446 compartments as part of a conservative mass relation, the isotopic composition of reagents and products
447 of the burning can be described by the mass balance given in Equation 3.

448

$$449 \overline{(EF_{Soil} * CI_{Soil0-1cm})} + \overline{(EF_{biomass} * CI_{biomass})} = \overline{(Hg_{ash} * CI_{ash})} + \overline{EF_{Atm} * CI_{Atm}} \quad (3)$$

450 Where:

451 $\overline{EF_{Soil}}$ = Average mass of Hg emitted by soils (in μg of Hg per m^2);

452 $\overline{EF_{Biomass}}$ = Average mass of Hg emitted by biomass (in μg of Hg per m^2);

453 $\overline{Hg_{ash}}$ = Average mass of Hg remaining in ash (in μg of Hg per m^2);

454 \overline{EF}_{Atm} = Average mass of total Hg emitted to the atmosphere due to forest burning (sum of all emitted
 455 species (GEM, PBM, etc.), in μg of Hg per m^2);

456 \overline{IC}_X = estimated average isotopic composition $\delta^{202}\text{Hg}$, $\Delta^{199}\text{Hg}$, $\Delta^{200}\text{Hg}$ for each studied matrix (where
 457 X is the soil, biomass, ash or atmosphere) (in ‰).

458

459 The detail of the calculations performed to obtain these different masses is presented in the SI
 460 (Text S3). By considering Equation 3 as an acceptable first approximation and using the different
 461 values obtained for Hg average isotopic composition of each compartment (Table 2) together with the
 462 average EF or remaining mass (Table S11) in each compartment, we estimate the average isotopic
 463 composition of the atmospheric Hg emissions presented in Table 3.

464

465 **Table 3.** Average Hg isotopic composition obtained for soils, litter and ash and calculated for the
 466 atmospheric emissions due to the Candeias do Jamari experimental burn

467

Compartment (mean \pm 1SD)				
Isotopes	0-1-cm soil layer			
	before burning (N=5)	Litter (N=9)	Ash (N=9)	Atmosphere
$\delta^{202}\text{Hg}$ (‰)	-2.02 ± 0.14	-1.63 ± 0.16	-1.78 ± 0.10	-1.79 ± 0.24
$\Delta^{200}\text{Hg}$ (‰)	-0.02 ± 0.01	-0.07 ± 0.04	-0.03 ± 0.02	-0.05 ± 0.04
$\Delta^{199}\text{Hg}$ (‰)	-0.58 ± 0.02	-0.37 ± 0.05	-0.58 ± 0.06	-0.45 ± 0.12

468

469 Up to now, studies on Hg isotopic composition due to combustion processes were only
470 performed for coal (Sun et al., 2014; Tang et al., 2017; Sun, 2019). For global coal, Sun et al. (2014)
471 reported $\delta^{202}\text{Hg} = -1.2 \pm 0.5\text{‰}$ (1SD). For coals from different locations these authors concluded that
472 due to the variability of $\delta^{202}\text{Hg}$ between different coals, their emissions could result in different $\delta^{202}\text{Hg}$,
473 reflecting the high variability observed in various locations (1SD=0.5‰). Considering that the isotopic
474 composition of plants and soils varies depending on the location, type of plant, climatic conditions,
475 among other factors (Demers et al., 2013; Fu et al., 2019), significant uncertainties can also be expected
476 for the isotopic composition of Hg emissions from forest fires. The relatively high uncertainty obtained
477 for the estimated isotopic composition of the Hg emitted to the atmosphere in this study (Table 3) is
478 therefore consistent and overlaps with the expected variability for Hg emissions for different types of
479 forest fire. The present estimate can therefore be considered as an initial fingerprint of atmospheric Hg
480 isotopic composition resulting from forest fire.

481

482 **Conclusion**

483

484 The results obtained indicate that a burnt forest is a complex environment, with Hg emissions
485 being affected by several parameters. Mercury bound to litter is mostly emitted to the atmosphere,
486 while soil Hg may be partially emitted, varying accordingly to the burning conditions. In this way, Hg
487 isotopic fractionation was determined during forest fires but may occur at very different extent. Several
488 factors may act altogether, influencing the Hg isotopic composition in the fuels and the burning process
489 itself. Based on our findings, we conclude that Hg isotopic fractionation may occur during forest
490 burning, mainly following MDF, while no significant MIF variations can be observed. To better
491 understand Hg emissions and isotopic fractionation processes due to forest burning more studies should
492 be performed in different areas and types of forests, but also the influence of fuel and burning
493 conditions should be investigated in controlled conditions.

494 **Acknowledgements**

495

496 This work was funded by The São Paulo Research Foundation (FAPESP) (Projects 2008/04490-4,
497 2010/19040-4, 2014/00555-5 and 2016/14227-5) and also partially funded by the Regional Council of
498 Nouvelle Aquitaine (France) and French National Research Agency (ANR). Larissa Richter received
499 a fellowship from the Brazilian Coordination for the Improvement of Higher Education Personnel,
500 CAPES, (Financing code 001). We also thank the Brazilian Environmental Secretary for authorizing
501 the experiments that enabled this work. For the experimental work, we thank the owners of the Caiabi
502 Farm, the co-workers from the Brazilian Institute of Environment and Renewable Natural Resources
503 (IBAMA) and the Brazilian National Institute of Spatial Research (INPE). This work is a contribution
504 to the European MercOx project (EMPIR EURAMET, Grant number 16ENV01). Jim Hesson
505 copyedited the manuscript (<https://www.academicenglishsolutions.com/editing-service>).

506

507 **References**

- 508 Abraham, J., Dowling, K., Florentine, S. (2018). Effects of prescribed fire and post-fire rainfall on
509 mercury mobilization and subsequent contamination assessment in a legacy mine site in Victoria,
510 Australia. *Chemosphere* 190, 144-153.
- 511 Almeida, M.D., Lacerda, L.D., Bastos, W.R., and Herrmann, J.C. (2005). Mercury loss from soils
512 following conversion from forest to pasture in Rondonia, Western Amazon, Brazil. *Environmental*
513 *Pollution* 137, 179-186.
- 514 Aparecido, L.E.D., De Moraes, J.R.D.C., De Meneses, K.C., Torsoni, G.B., De Lima, R.F., and
515 Costa, C.T.S. (2020). Koppen-Geiger and Camargo climate classifications for the Midwest of
516 Brasil. *Theoretical and Applied Climatology* 142, 1133-1145.

517 Araujo, B.F., Hintelmann, H., Dimock, B., De Lima Sobrinho, R., Bernardes, M.C., De Almeida,
518 M.G., Krusche, A.V., Rangel, T.P., Thompson, F., and De Rezende, C.E. (2018). Mercury
519 speciation and Hg stable isotope ratios in sediments from Amazon floodplain lakes—Brazil. 63,
520 1134-1145.

521 Barre, J.P.G., Deletraz, G., Sola-Larranaga, C., Santamaria, J.M., Berail, S., Donard, O.F.X., and
522 Amouroux, D. (2018). Multi-element isotopic signature (C, N, Pb, Hg) in epiphytic lichens to
523 discriminate atmospheric contamination as a function of land-use characteristics (Pyrenees-
524 Atlantiques, SW France). *Environmental Pollution* 243, 961-971.

525 Barre, J.P.G., Queipo-Abad, S., Sola-Larrañaga, C., Deletraz, G., Bérail, S., Tessier, E., Elustondo
526 Valencia, D., Santamaría, J.M., De Diego, A., and Amouroux, D. (2020). Comparison of the
527 Isotopic Composition of Hg and Pb in Two Atmospheric Bioaccumulators in a Pyrenean Beech
528 Forest (Iraty Forest, Western Pyrenees, France/Spain). 1.

529 Bergquist, B.A., and Blum, J.D. (2007). Mass-dependent and mass-independent fractionation of Hg
530 isotopes in aquatic systems. *Geochimica Et Cosmochimica Acta* 71, A83-A83.

531 Bishop, K., Shanley, J.B., Riscassi, A., De Wit, H.A., Eklof, K., Meng, B., Mitchell, C., Osterwalder,
532 S., Schuster, P.F., Webster, J., and Zhu, W. (2020). Recent advances in understanding and
533 measurement of mercury in the environment: Terrestrial Hg cycling. *Science of the Total*
534 *Environment* 721.

535 Blum, J.D., Sherman, L.S., and Johnson, M.W. (2014). Mercury Isotopes in Earth and Environmental
536 Sciences. *Annual Review of Earth and Planetary Sciences, Vol 42* 42, 249-269.

537 Brown, I.F., Martinelli, L.A., Thomas, W.W., Moreira, M.Z., Ferreira, C.a.C., and Victoria, R.A.
538 (1995). Uncertainty in the Biomass of Amazonian Forests - an Example from Rondonia, Brazil.
539 *Forest Ecology and Management* 75, 175-189.

540 Carmenta, R., Parry, L., Blackburn, A., Vermeulen, S., and Barlow, J. (2011). Understanding
541 Human-Fire Interactions in Tropical Forest Regions: a Case for Interdisciplinary Research across
542 the Natural and Social Sciences. *Ecology and Society* 16.

543 Carvalho, J.A., Costa, F.S., Veras, C.a.G., Sandberg, D.V., Alvarado, E.C., Gielow, R., Serra, A.M.,
544 and Santos, J.C. (2001). Biomass fire consumption and carbon release rates of rainforest-clearing
545 experiments conducted in northern Mato Grosso, Brazil. *Journal of Geophysical Research-*
546 *Atmospheres* 106, 17877-17887.

547 Certini, G. (2005). Effects of fire on properties of forest soils: a review. *Oecologia* 143, 1-10.

548 Chave, J., Navarrete, D., Almeida, S., Alvarez, E., Aragao, L.E.O.C., Bonal, D., Chatelet, P., Silva-
549 Espejo, J.E., Goret, J.Y., Von Hildebrand, P., Jimenez, E., Patino, S., Penuela, M.C., Phillips,
550 O.L., Stevenson, P., and Malhi, Y. (2010). Regional and seasonal patterns of litterfall in tropical
551 South America. *Biogeosciences* 7, 43-55.

552 Chen, C., Wang, H.H., Zhang, W., Hu, D., Chen, L., and Wang, X.J. (2013). High-resolution
553 inventory of mercury emissions from biomass burning in China for 2000-2010 and a projection for
554 2020. *Journal of Geophysical Research-Atmospheres* 118, 12248-12256.

555 De Simone, F., Artaxo, P., Bencardino, M., Cinnirella, S., Carbone, F., D'amore, F., Dommergue, A.,
556 Feng, X.B., Gencarelli, C.N., Hedgecock, I.M., Landis, M.S., Sprovieri, F., Suzuki, N., Wangberg,
557 I., and Pirrone, N. (2017). Particulate-phase mercury emissions from biomass burning and impact
558 on resulting deposition: a modelling assessment. *Atmospheric Chemistry and Physics* 17, 1881-
559 1899.

560 De Simone, F., Cinnirella, S., Gencarelli, C.N., Yang, X., Hedgecock, I.M., and Pirrone, N. (2015).
561 Model Study of Global Mercury Deposition from Biomass Burning. *Environmental Science &*
562 *Technology* 49, 6712-6721.

563 Demers, J.D., Blum, J.D., and Zak, D.R. (2013). Mercury isotopes in a forested ecosystem:
564 Implications for air-surface exchange dynamics and the global mercury cycle. *Global*
565 *Biogeochemical Cycles* 27, 222-238.

566 Engle, M.A., Gustin, M.S., Johnson, D.W., Murphy, J.F., Miller, W.W., Walker, R.F., Wright, J., and
567 Markee, M. (2006). Mercury distribution in two Sierran forest and one desert sagebrush steppe
568 ecosystems and the effects of fire. *Science of the Total Environment* 367, 222-233.

569 Enrico, M., Le Roux, G., Maruszczak, N., Heimburger, L.E., Claustres, A., Fu, X.W., Sun, R.Y., and
570 Sonke, J.E. (2016). Atmospheric Mercury Transfer to Peat Bogs Dominated by Gaseous
571 Elemental Mercury Dry Deposition. *Environmental Science & Technology* 50, 2405-2412.

572 Feinberg, A., T. Dlamini, M. Jiskra, V. Shah, and N. E. Selin. 2022. Evaluating atmospheric mercury
573 (Hg) uptake by vegetation in a chemistry-transport model. *Environmental Science: Processes &*
574 *Impacts*. Royal Society of Chemistry. doi:10.1039/D2EM00032F.

575 Ferraz, S.F.D., Vettorazzi, C.A., Theobald, D.M., and Ballester, M.V.R. (2005). Landscape dynamics
576 of Amazonian deforestation between 1984 and 2002 in central Rondonia, Brazil: assessment and
577 future scenarios. *Forest Ecology and Management* 204, 67-83.

578 Fostier, A.H., Melendez-Perez, J.J., and Richter, L. (2015). Litter mercury deposition in the
579 Amazonian rainforest. *Environmental Pollution* 206, 605-610.

580 Friedli, H.R., Arellano, A.F., Cinnirella, S., and Pirrone, N. (2009). Initial Estimates of Mercury
581 Emissions to the Atmosphere from Global Biomass Burning. *Environmental Science &*
582 *Technology* 43, 3507-3513.

583 Fu, X., Zhang, H., Liu, C., Zhang, H., Lin, C.-J., and Feng, X. (2019). Significant Seasonal
584 Variations in Isotopic Composition of Atmospheric Total Gaseous Mercury at Forest Sites in
585 China Caused by Vegetation and Mercury Sources. *Environmental Science & Technology* 53,
586 13748-13756.

587 González-Pérez, J.A., González-Vila, F.J., Almendros, G., and Knicker, H. (2004). The effect of fire
588 on soil organic matter--a review. *Environment international* 30, 855-870.

589 Guedron, S., Arnouroux, D., Tessier, E., Grimaldi, C., Barre, J., Berail, S., Perrot, V., and Grimaldi,
590 M. (2018). Mercury Isotopic Fractionation during Pedogenesis in a Tropical Forest Soil Catena
591 (French Guiana): Deciphering the Impact of Historical Gold Mining. *Environmental Science &*
592 *Technology* 52, 11573-11582.

593 Gustin, M.S., Huang, J.Y., Miller, M.B., Peterson, C., Jaffe, D.A., Ambrose, J., Finley, B.D., Lyman,
594 S.N., Call, K., Talbot, R., Feddersen, D., Mao, H.T., and Lindberg, S.E. (2013). Do We
595 Understand What the Mercury Speciation Instruments Are Actually Measuring? Results of
596 RAMIX. *Environmental Science & Technology* 47, 7295-7306.

597 Gworek, B., Dmuchowski, W., and Baczevska-Dabrowska, A.H. (2020). Mercury in the terrestrial
598 environment: a review. *Environmental Sciences Europe* 32.

599 Hintelmann, H., and Zheng, W. (2011). "Tracking Geochemical Transformations and Transport of
600 Mercury through Isotope Fractionation," in *Environmental Chemistry and Toxicology of Mercury*,
601 eds. G. Liu, Y. Cai & N. O'driscoll.), 293-327.

602 INPE (2022). *Monitoramento do Desmatamento da Floresta Amazônica Brasileira por Satélite*
603 [Online]. Available: <http://www.obt.inpe.br/OBT/assuntos/programas/amazonia/prodes>
604 [Accessed].

605 Jiskra, M., Sonke, J.E., Obrist, D., Bieser, J., Ebinghaus, R., Myhre, C.L., Pfaffhuber, K.A.,
606 Wangberg, I., Kyllonen, K., Worthy, D., Martin, L.G., Labuschagne, C., Mkololo, T., Ramonet,
607 M., Magand, O., and Dommergue, A. (2018). A vegetation control on seasonal variations in global
608 atmospheric mercury concentrations. *Nature Geoscience* 11, 244-+.

609 Jiskra, M., Wiederhold, J.G., Skyllberg, U., Kronberg, R.M., Hajdas, I., and Kretzschmar, R. (2015).
610 Mercury Deposition and Re-emission Pathways in Boreal Forest Soils Investigated with Hg
611 Isotope Signatures. *Environmental Science & Technology* 49, 7188-7196.

612 Kato, S., Akimoto, H., Röckmann, T., Bräunlich, M., and Brenninkmeijer, C.a.M. (1999). Stable
613 isotopic compositions of carbon monoxide from biomass burning experiments. *Atmospheric*
614 *Environment* 33, 4357-4362.

615 Keeley, J.E., Safford, H., Fotheringham, C.J., Franklin, J., and Moritz, M. (2009). The 2007 Southern
616 California Wildfires: Lessons in Complexity. *Journal of Forestry* 107, 287-296.

617 Kendall, C., and Doctor, D.H. (2003). "5.11 - Stable Isotope Applications in Hydrologic Studies," in
618 *Treatise on Geochemistry*, eds. H.D. Holland & K.K. Turekian. (Oxford: Pergamon), 319-364.

619 Kumar, A., Wu, S.L., Huang, Y.X., Liao, H., and Kaplan, J.O. (2018). Mercury from wildfires:
620 Global emission inventories and sensitivity to 2000-2050 global change. *Atmospheric*
621 *Environment* 173, 6-15.

622 Kwon, S.Y., Blum, J.D., Yin, R., Tsui, M.T-K, Yang, Y.O., Choi, J.W. (2020). Mercury stable
623 isotopes for monitoring the effectiveness of the Minamata Convention on Mercury. *Earth-Science*
624 *Reviews* 203, 103111.

625 Lacerda, L.D., De Souza, M., and Ribeiro, M.G. (2004). The effects of land use change on mercury
626 distribution in soils of Alta Floresta, Southern Amazon. *Environmental Pollution* 129, 247-255.

627 Li, X.Y., Li, Z.G., Chen, J., Zhang, L.M., Yin, R.S., Sun, G.Y., Meng, B., Cui, Z.K., and Feng, X.B.
628 (2021). Isotope signatures of atmospheric mercury emitted from residential coal combustion.
629 *Atmospheric Environment* 246.

630 Liu, H.-W., Shao, J.-J., Yu, B., Liang, Y., Duo, B., Fu, J.-J., Yang, R.-Q., Shi, J.-B., and Jiang, G.-B.
631 (2019). Mercury isotopic compositions of mosses, conifer needles, and surface soils: Implications
632 for mercury distribution and sources in Shergyla Mountain, Tibetan Plateau. *Ecotoxicology and*
633 *Environmental Safety* 172, 225-231.

634 Mataix-Solera, J., Cerda, A., Arcenegui, V., Jordan, A., and Zavala, L.M. (2011). Fire effects on soil
635 aggregation: A review. *Earth-Science Reviews* 109, 44-60.

636 Melendez-Perez, J.J., and Fostier, A.H. (2013). Assessment of direct Mercury Analyzer® to quantify
637 mercury in soils and leaf samples. *Journal of the Brazilian Chemical Society* 24, 1880-1886.

638 Melendez-Perez, J.J., Fostier, A.H., Carvalho, J.A., Windmoller, C.C., Santos, J.C., and Carpi, A.
639 (2014). Soil and biomass mercury emissions during a prescribed fire in the Amazonian rain forest.
640 *Atmospheric Environment* 96, 415-422.

641 Merino et al. (2018). Inferring changes in soil organic matter in post-wildfire soil burn severity levels
642 in a temperate climate. *Science of the Total Environment* 627 (2018) 622–632.

643 Michelazzo, P.a.M., Fostier, A.H., Magarelli, G., Santos, J.C., and De Carvalho, J.A. (2010).
644 Mercury emissions from forest burning in southern Amazon. *Geophysical Research Letters* 37.

645 Miserendino, R.A., Guimardes, J.R.D., Schudel, G., Ghosh, S., Godoy, J.M., Silbergeld, E.K., Lees,
646 P.S.J., and Bergquist, B.A. (2018). Mercury Pollution in Amapa, Brazil: Mercury Amalgamation
647 in Artisanal and Small-Scale Gold Mining or Land-Cover and Land-Use Changes? *Earth and*
648 *Space Chemistry* 2, 441-450.

649 North Central Regional Research, N. (2012). "Recommended Chemical Soil Test Procedures for the
650 North Central Region". (United States of America: North Central Regional Research).

651 Obrist, D., Kirk, J.L., Zhang, L., Sunderland, E.M., Jiskra, M., and Selin, N.E. (2018). A review of
652 global environmental mercury processes in response to human and natural perturbations: Changes
653 of emissions, climate, and land use. *Ambio* 47, 116-140.

654 Outridge, P.M., Mason, R.P., Wang, F., Guerrero, S., and Heimbürger-Boavida, L.E. (2018).
655 Updated Global and Oceanic Mercury Budgets for the United Nations Global Mercury
656 Assessment 2018. *Environmental Science & Technology* 52, 11466-11477.

657 Schudel, G., Miserendino, R.A., Veiga, M.M., Velasquez-López, P.C., Lees, P.S.J., Winland-Gaetz,
658 S., Davée Guimarães, J.R., and Bergquist, B.A. (2018). An investigation of mercury sources in the
659 Puyango-Tumbes River: Using stable Hg isotopes to characterize transboundary Hg pollution.
660 *Chemosphere* 202, 777-787.

661 Schumacher, M., Werner, R.A., Meijer, H.a.J., Jansen, H.G., Brand, W.A., Geilmann, H., and
662 Neubert, R.E.M. (2011). Oxygen isotopic signature of CO₂ from combustion
663 processes. *Atmospheric Chemistry and Physics* 11, 1473-1490.

664 Shi, Y.S., Zhao, A.M., Matsunaga, T., Yamaguchi, Y., Zang, S.Y., Li, Z.Q., Yu, T., and Gu, X.F.
665 (2019). High-resolution inventory of mercury emissions from biomass burning in tropical
666 continents during 2001-2017. *Science of the Total Environment* 653, 638-648.

667 Sun, R., Sonke, J.E., Heimbürger, L.-E., Belkin, H.E., Liu, G., Shome, D., Cukrowska, E., Lioussé,
668 C., Pokrovsky, O.S., and Streets, D.G. (2014). Mercury Stable Isotope Signatures of World Coal
669 Deposits and Historical Coal Combustion Emissions. *Environmental Science & Technology* 48,
670 7660-7668.

671 Sun, R.Y. (2019). Mercury Stable Isotope Fractionation During Coal Combustion in Coal-Fired
672 Boilers: Reconciling Atmospheric Hg Isotope Observations with Hg Isotope Fractionation Theory.
673 *Bulletin of Environmental Contamination and Toxicology* 102, 657-664.

674 Tang, S., Feng, C., Feng, X., Zhu, J., Sun, R., Fan, H., Wang, L., Li, R., Mao, T., and Zhou, T.
675 (2017). Stable isotope composition of mercury forms in flue gases from a typical coal-fired power
676 plant, Inner Mongolia, northern China. *Journal of Hazardous Materials* 328, 90-97.

677 Wang, X., Bao, Z.D., Lin, C.J., Yuan, W., and Feng, X.B. (2016). Assessment of Global Mercury
678 Deposition through Litterfall. *Environmental Science & Technology* 50, 8548-8557.

679 Wang, X., Luo, J., Yin, R.S., Yuan, W., Lin, C.J., Sommar, J., Feng, X.B., Wang, H.M., and Lin, C.
680 (2017). Using Mercury Isotopes To Understand Mercury Accumulation in the Montane Forest
681 Floor of the Eastern Tibetan Plateau. *Environmental Science & Technology* 51, 801-809.

682 Wang, X., Yuan, W., Lin, C.-J., Zhang, L., Zhang, H., and Feng, X. (2019). Climate and Vegetation
683 As Primary Drivers for Global Mercury Storage in Surface Soil. *Environmental Science &*
684 *Technology* 53, 10665-10675.

685 Wang, X., Yuan, W., Lin, C.-J., Feng, X. (2021). Mercury cycling and isotopic fractionation in
686 global forests. *Critical Reviews in Environmental Science and Technology*.

687 Witt, E.L., Kolka, R.K., Nater, E.A., Wickman, T.R.J.W., Air,, and Pollution, S. (2009). Influence of
688 the Forest Canopy on Total and Methyl Mercury Deposition in the Boreal Forest. *Water Air and*
689 *Soil Pollution* 199, 3-11.

690 Yuan, W., Sommar, J., Lin, C.-J., Wang, X., Li, K., Liu, Y., Zhang, H., Lu, Z., Wu, C., and Feng, X.
691 (2019). Stable Isotope Evidence Shows Re-emission of Elemental Mercury Vapor Occurring after
692 Reductive Loss from Foliage. *Environmental Science & Technology* 53, 651-660.

693 Zhang, H., Yin, R.S., Feng, X.B., Sommar, J., Anderson, C.W.N., Sapkota, A., Fu, X.W., and
694 Larssen, T. (2013). Atmospheric mercury inputs in montane soils increase with elevation:
695 evidence from mercury isotope signatures. *Scientific Reports* 3.

696 Zheng, W., Obrist, D., Weis, D., and Bergquist, B.A. (2016). Mercury isotope compositions across
697 North American forests. *Global Biogeochemical Cycles* 30, 1475-1492.

698 Zhou, J., Obrist, D., Dastoor, A., Jiskra, M., and Ryjkov, A. (2021). Vegetation uptake of mercury
699 and impacts on global cycling. *Nature Reviews Earth & Environment* 2, 269-284.

700



[Click here to access/download](#)

Supplementary Material

[Richter et al. -Supplementary Information.docx](#)

